

# REPORT DOCUMENT P

# AD-A276 389

v. 2-89)

2

Public reporting burden for the collection of information is estimated to average 1 hour and maintaining the data needed, and completing and reviewing the collection of information, including suggestions for reducing this burden to Washington Headquarters, 1215 Jefferson Avenue, Arlington, VA 22202-4302, and to the Office of Management and Budget, Paperwork Project, Washington, DC 20503.

ing data sources, gathering aspect of the collection of road Davis Highway, Suite

1. AGENCY USE ONLY (Leave blank)		2. REPORT DATE 13 JAN 1994		3. REPORT TYPE AND DATES COVERED Interim technical report	
4. TITLE AND SUBTITLE New Material for High Average Power Infrared Generation: QPM-DB GaAs				5. FUNDING NUMBERS DAAL03-92-G-0400	
6. AUTHORS L. Gordon, R. C. Eckardt, R. L. Byer, R. K. Route and R. S. Feigelson					
7. PERFORMING ORGANIZATION NAME(S) AND ADDRESSES Ginzton Laboratory, Stanford University Stanford, CA 94305-4085				8. PERFORMING ORGANIZATION REPORT NUMBER GL 5133	
9. SPONSORING/MONITORING AGENCY NAME(S) AND ADDRESS(ES) U.S. Army Research Office P.O. Box 1211 Research Triangle Park, NC 27709-2211				10. SPONSORING/MONITORING AGENCY REPORT NUMBER ARO 30708.2-PH	
11. SUPPLEMENTARY NOTES  The view, opinions and/or findings contained in this report are those of the author(s) and should not be construed as an official Department of the Army position, policy, or decision, unless so designated by other documentation.					
12a. DISTRIBUTION/AVAILABILITY STATEMENT Approved for public release; distribution unlimited.				12b. DISTRIBUTION CODE	
13. ABSTRACT (Maximum 200 words)  We are investigating quasi-phase-matched diffusion-bonded (QPM-DB) GaAs for nonlinear infrared applications. We have fabricated diffusion-bonded stacks of up to nine layers, which we have used to demonstrate quasi-phase-matched second-harmonic generation pumped by 10.6- $\mu\text{m}$ CO <sub>2</sub> laser output. Preliminary optical damage tests of diffusion-bonded-stacked GaAs indicate a power handling capability in excess of other currently available nonlinear infrared materials. Numerical calculations modeling nonlinear frequency conversion and projected device performance are included in this report.					
14. SUBJECT TERMS optics, lasers, nonlinear infrared frequency conversion, GaAs, diffusion bonding				15. NUMBER OF PAGES 32	
				16. PRICE CODE	
17. SECURITY CLASSIFICATION OF REPORT UNCLASSIFIED		18. SECURITY CLASSIFICATION OF THIS PAGE UNCLASSIFIED		19. SECURITY CLASSIFICATION OF ABSTRACT UNCLASSIFIED	
				20. LIMITATION OF ABSTRACT UL	

DTIC  
1994



**New Material for High Average Power  
Infrared Generation: QPM-DB GaAs**

Technical report submitted to the  
U. S. Army Research Office

L. Gordon, R. C. Eckardt, R. L. Byer,  
R. K. Route and R. S. Feigelson

Center for Nonlinear Optical Materials  
Ginzton Laboratory  
Stanford University  
Stanford, CA 94305-4085

January 12, 1994

**Abstract**

We are investigating quasi-phase-matched diffusion-bonded (QPM-DB) GaAs for nonlinear infrared applications. We have fabricated diffusion-bonded stacks of up to nine layers, which we have used to demonstrate quasi-phase-matched second-harmonic generation pumped by 10.6- $\mu\text{m}$  CO<sub>2</sub> laser output. Preliminary optical damage tests of diffusion-bonded-stacked GaAs indicate a power handling capability in excess of other currently available nonlinear infrared materials. Numerical calculations modeling nonlinear frequency conversion and projected device performance are included in this report.

THE VIEWS, OPINIONS, AND/OR FINDINGS CONTAINED IN THIS REPORT ARE THOSE OF THE AUTHOR AND SHOULD NOT BE CONSTRUED AS AN OFFICIAL DEPARTMENT OF THE ARMY POSITION, POLICY, OR DECISION, UNLESS SO DESIGNATED BY OTHER DOCUMENTATION.

103

**Diffusion-Bonded Nonlinear Materials  
for Practical Quasi-Phase-Matched Mid-IR Devices**

**Table of Contents**

Abstract .....	ii
Table of Contents .....	iii
I. Introduction .....	1
II. Background .....	2
A. Quasi phase matching .....	2
B. Historical overview .....	3
C. Materials issues .....	4
III. Progress in diffusion bonding of GaAs for QPM interactions .	6
A. Diffusion bonding investigations .....	6
B. Demonstration of phase-coherent SHG .....	9
C. Preliminary damage measurements .....	9
D. Coherence length and tolerance calculations .....	10
E. Calculations of frequency conversion .....	13
IV. Future Research .....	21
A. Material processing studies .....	21
B. Characterization .....	22
C. Theory .....	23
D. Devices .....	23
V. Relationship to other programs .....	25
VI. Scientific Personnel Supported by this Contract .....	26
VI. References .....	26

## **New Material for High Average Power Infrared Generation: QPM-DB GaAs**

Technical Report submitted to the  
U. S. Army Research Office

L. Gordon, R. C. Eckardt, R. L. Byer  
R. K. Route and R. S. Feigelson

### **I. Introduction**

There is strong motivation for developing a new class of nonlinear materials for infrared (IR) applications that require nonlinear frequency conversion. These applications include laboratory spectroscopy, remote sensing, detection and illumination, and satellite observation of the earth for meteorological and atmospheric compositional information. The average power and peak power limitations of existing nonlinear IR materials have restricted performance in the nonlinear frequency conversion of the output of existing lasers such as Nd:YAG at 1.06- $\mu\text{m}$ , Ho:YAG and Tm:YAG at 2  $\mu\text{m}$ , and CO<sub>2</sub> at 10- $\mu\text{m}$ . These limitations are due to optical loss, low damage thresholds, and the thermal/mechanical properties of the existing nonlinear materials.

We are investigating diffusion bonding of GaAs and related materials to meet the requirements for IR sources. We have made preliminary studies that are quite promising. The studies include fabrication of diffusion-bonded GaAs structures from 2 to 9 layers in thickness and the demonstration of quasi-phase-matched (QPM) second-harmonic generation (SHG) in these devices [1,2]. We have made initial damage measurements that were encouraging but limited by degradation of the exterior surfaces that occurred during the diffusion bonding process. We now have the capability to polish GaAs, which allows us to prepare wafers to the desired thickness and repolish the external surfaces after bonding. In the work reported here, we have also surveyed other nonlinear materials and have modeled nonlinear frequency conversion in devices. The continuing investigation will build on the preliminary results with laboratory demonstrations of practical nonlinear mid-IR devices emphasizing mid-IR optical parametric oscillators (OPO's).

This is a collaborative research program in the Center for Nonlinear Optical Materials at Stanford University. Professor Byer is the principal investigator and is responsible for coordinating efforts and for investigations of device development and optical characterization of materials. Professor Feigelson performs investigations related to material processing. We also have collaborated with researchers outside of Stanford on damage measurements. Further collaborative efforts are planned with the Naval Command Control and Ocean Surveillance Center (NRaD) involving joint research for material evaluation and device testing, and with other organizations on various aspects of material development.

In section II of this report we present a brief background summary for this research program that includes a short technical description of QPM processes and reviews of QPM history and materials issues. The progress of our investigation of diffusion-bonded GaAs is discussed in Section III. Future work for this investigation is presented in Section IV followed by a discussion of the relationship of this program to other current research programs under the direction of Professor Byer.

## II. Background

### A. *Quasi phase matching*

Currently there are no tunable high power sources in the mid infrared atmospheric window bands. Applications in remote sensing require tunable infrared sources in the 3- to 5- $\mu\text{m}$  spectral region with 10- to 100-W average power in a repetitively pulsed output. There are well developed lasers adjacent to this spectral region, namely the Nd:YAG laser at 1.06  $\mu\text{m}$  and the CO<sub>2</sub> laser at 10.6  $\mu\text{m}$ . Recently Tm: and Ho:YAG lasers at 2  $\mu\text{m}$  have been demonstrated with good performance. Nonlinear frequency conversion systems pumped by these lasers and providing output throughout IR would be most useful. However, existing nonlinear IR materials such as the chalcopyrites AgGaSe<sub>2</sub> or ZnGeP<sub>2</sub> show average-power limitations due to low damage thresholds or high absorption. A new nonlinear material with the power handling capabilities of bulk GaAs or ZnSe would allow power scaling to levels that are well beyond the current limits..

Materials with the zinc-blend structure such as GaAs or ZnSe, however, are not birefringent, and conventional birefringent phase-matching techniques can not be used. Typically these materials have coherence lengths of tens of  $\mu\text{m}$  to more than 100  $\mu\text{m}$ . The coherence length  $l_c$  is the distance of propagation in the material over which the relative phase of the interacting waves changes by  $\pi$  radians. The coherence length is determined by the wave vector mismatch  $\Delta k$  of the bulk material, that is

$$l_c = \pi / \Delta k, \quad \text{where}$$

$$\Delta k = k_{2\omega} - 2k_\omega \text{ for SHG}$$

or

$$\Delta k = k_3 - k_1 - k_2 \text{ for 3-wave processes.}$$

The magnitudes of the wave vectors are given by  $k = 2\pi n/\lambda$ , where  $n$  is the refractive index and  $\lambda$  is the free space wavelength. With each  $\pi$  change of relative phase, the energy flow of the nonlinear frequency conversion process reverses, and only an oscillating, low-efficiency conversion is attained with propagation through the material. However, if the sign of the nonlinear coefficient is reversed every coherence length, then the energy conversion continues. This approach to phase matching is called quasi phase matching and was first proposed by Bloembergen in 1962 [3].

Optimally, in a quasi-phase-matched (QPM) material, the sign of the optical nonlinearity is reversed once every coherence length, but it can also be done an odd multiples of the coherence length. The number of coherence lengths that is used is the QPM order, and it is identified with an integer  $m$ . Many of the frequency conversion relationships for conventional phase matching can be applied to quasi phase matching if the effective nonlinear coefficient is properly defined. The effective nonlinear coefficient for a QPM process is reduced by a factor of  $2/m\pi$  from the effective nonlinear coefficient of single crystal bulk material [4], that is

$$d_Q = 2d_{\text{eff}} / (m\pi).$$

It is possible to define a wavevector mismatch associated with the QPM material. For the ideal case where the alternating layers have the same thickness  $l$ , the wavevector mismatch of a QPM material of order  $m$  is

$$\Delta k_Q = \Delta k - m\pi/l.$$

There is a large range of conditions over which QPM frequency conversion can be represented by the models developed for single-domain materials with parameters adjusted for quasi phase matching, but caution is required at high conversion levels as shown in subsection III.E.

### *B. Historical overview*

Quasi phase matching was first proposed in 1962 [3]. It has been analyzed theoretically [4-6], and demonstrated in air-spaced stacks of GaAs plates [7, 8], and it is now extensively used in waveguide structures. Techniques such as metal indiffusion are used for creating closely spaced domains (3-20  $\mu\text{m}$ ) in ferroelectric materials such as  $\text{LiNbO}_3$  [9, 10]. Recently, domains have been grown in ZnSe and ZnTe with MOCVD

after patterning the substrate with CdTe [11]. Plates of  $\text{LiB}_3\text{O}_5$  250- $\mu\text{m}$  thick have been optically contacted in QPM stacks with good results [12].

With stacks of plates of III-V and II-VI materials, it is possible to alternate the sign of the nonlinear coefficient by an appropriate rotation of the individual plates. The air-spaced stacks of plates used in the early work had excessive losses due to the high index of refraction of these materials. This was true even with Brewster's angle incidence because of the large number of plates required. We have proposed and are performing an investigation of the use of diffusion bonding to reduce losses at the interfaces between the plates and retain the optical, mechanical, and thermal properties of the bulk materials.

It has been shown [13-15] that III-V semiconductor wafers of similar composition, or different compositions, can be bonded together at elevated temperatures under modest pressure to give an electronic structure comparable in performance to that achieved by thin film epitaxy. This technique has been called wafer fusion, wafer bonding or bonding by atomic rearrangement as well as diffusion bonding. Bonding was found to be uniform over the small regions examined by the early researchers, but long range variations in bonding uniformity and the presence of grain boundary pores (interfacial voids) have not been studied extensively.

### *C. Materials issues*

For nonlinear optical applications, the problem is more complex than for the electronic semiconductor structures demonstrated by the early researchers because QPM structures require the simultaneous bonding of a stack of perhaps 100 wafers. The reliability and predictability of the process must be high. It is clear that to make materials of suitable quality, we must develop a very thorough understanding of the bonding parameters and mechanisms involved in the bonding process.

In addition to investigation of the bonding process, we propose to extend the investigation to materials other than GaAs. Materials differ in transmission, dispersion, and optical nonlinearity as well as other physical and chemical properties. Different materials will be better choices for different applications. The dispersion properties of some materials that are possible choices for diffusion bonding applications are shown in Fig. 1. These curves were generated using dispersion equations given by Pikhtin and Yas'kov [16]. The regions of low dispersion near the center of the curves indicate the useful spectral region for that material.

Coherence length is an important parameter in choosing a material for QPM. Ideally, the coherence length should be as long as possible to simplify fabrication. We expect that it will be relatively straight forward to polish and handle wafers of approximately 100- $\mu\text{m}$  or

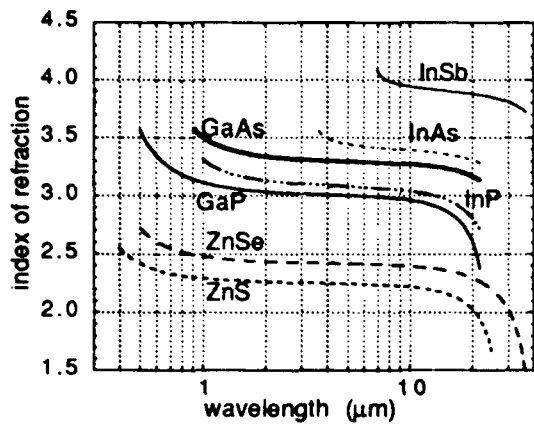


Fig. 1. Dispersion curves for III-V and II-VI semiconductor materials that are potentially useful in mid-IR nonlinear devices

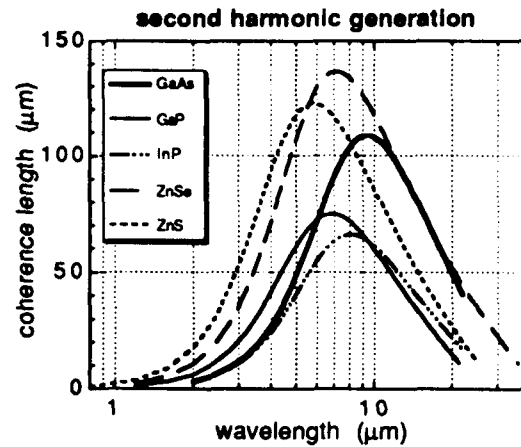


Fig. 2. Calculated coherence lengths for QPM SHG in some semiconductor materials. GaAs, ZnSe and ZnS look particularly promising in the 4 to 11- $\mu\text{m}$  spectral region.

TABLE I. Properties of some nonlinear semiconductors

material $\rightarrow$	GaAs	GaP	InSb	InAs	InP	ZnSe	$\beta$ -ZnS
$d_{14}$ (pm/V) source	83 Roberts	37 Roberts	500	300	140	50	25
transmission range ( $\mu\text{m}$ )	1-16	0.6-11	8-25	3.8-7	1-14	0.5-22	1-11
$\frac{dn}{dT}$ or $(1/n)\frac{dn}{dT}$ ( $^{\circ}\text{K}^{-1}$ )	$1.49 \times 10^{-4}$ @ 10 $\mu\text{m}$	$1.0 \times 10^{-4}$ @ 10 $\mu\text{m}$	$3.9 \times 10^{-5}$	$8.9 \times 10^{-5}$	$2.7 \times 10^{-5}$	$6.8 \times 10^{-5}$ @ 10 $\mu\text{m}$	$4.1 \times 10^{-5}$ @ 10 $\mu\text{m}$
$\frac{1}{L} \frac{dL}{dT}$ ( $^{\circ}\text{K}^{-1}$ )	$5.7 \times 10^{-6}$	$5.3 \times 10^{-6}$	$5.0 \times 10^{-6}$	$5.3 \times 10^{-6}$	$4.5 \times 10^{-6}$	$7.0 \times 10^{-6}$	$6.7 \times 10^{-6}$
$K$ (W/m $^{\circ}\text{K}$ )	52	110	36	50	70	18	27
$n$ @ 10 $\mu\text{m}$	3.27	2.96	3.95	3.42	3.05	2.41	2.28
$\alpha$ ( $\text{cm}^{-1}$ ) @ 10 $\mu\text{m}$	0.01	0.21	0.009	20	<0.1	0.0005	0.15

greater thickness. Coherence lengths for second-harmonic generation (SHG) calculated from the dispersion relationships are shown as a function of fundamental wavelength in Fig. 2. The materials GaAs, ZnSe, and ZnS are of particular interest because of greater than 100  $\mu\text{m}$  coherence length and good transmission in the mid infrared.

Some properties of GaAs are given in Tables 1 and 2 along with properties of some other nonlinear IR materials. The figure of merit  $d^2/(n^3\alpha^2)$  indicates the relative efficiency of nonlinear frequency conversion in a resonant cavity for the different materials when beam size and intensity are held constant. Here  $d$  is the effective nonlinear coefficient,  $n$  is the index of refraction, and  $\alpha$  is the absorption coefficient. We have measured damage thresholds in excess of 300 MW/cm<sup>2</sup> for GaAs using 200-ns-duration 10.6- $\mu\text{m}$  pulses, ten times greater than damage thresholds of other nonlinear infrared materials. The high damage threshold of GaAs is a distinct advantage. Nonlinear conversion efficiency is proportional to the square of the intensity, and a 10 times greater intensity translates to an additional 100 times increase in conversion efficiency. The tables provide a qualitative comparison of nonlinear materials because some parameters are not well known and other parameters such as absorption continue to improve with advances in growth technology. This qualitative comparison, however, clearly shows the potential advantage of diffusion-bonded materials such as GaAs for nonlinear infrared frequency conversion.

### III. Progress in diffusion bonding of GaAs for QPM interactions

We have built and tested several diffusion-bonded stacks of GaAs plates for 10.6- $\mu\text{m}$  quasi-phase-matched (QPM) second-harmonic generation (SHG). These monolithic structures retain the thermomechanical properties of the bulk material, and have been shown to be phase coherent over nine plates. We selected GaAs for the initial demonstration because inexpensive high-quality single-crystal wafers are commercially available. The {110} wafers were chosen for the SHG studies because they provided the maximum effective nonlinear coefficient in GaAs for normal incidence propagation. Available wafers were 435- $\mu\text{m}$  thick ( $\pm 5\text{-}\mu\text{m}$ ); while not an ideal multiple of the coherence length (106  $\mu\text{m}$  for SHG at 10.6  $\mu\text{m}$ ), they were adequate for initial testing of the diffusion bonding technique. We have also performed modeling calculations to project the performance of these devices.

#### A. Diffusion bonding investigations

Wafers were diced into 1-cm<sup>2</sup> pieces with edges lying along the  $\langle 100 \rangle$  and  $\langle 110 \rangle$  directions. After cleaning with trichloroethane followed by acetone and then methanol, the pieces were stacked between graphite spacers in a boron nitride holder in a clean room

TABLE II. Comparison of Figures of Merit for SHG in ZnGeP<sub>2</sub> and AgGaSe<sub>2</sub> and Diffusion-Bonded-Stacked (DBS) GaAs and ZnSe.

crystal	phase matching	$d_{\text{eff}}$ or $d_{\text{Q}}$ (pm/V)	absorption coefficient $\alpha_{\omega}$ (cm <sup>-1</sup> )	thermal conductivity $K$ (W/m <sup>2</sup> K)	$n_{\omega}$	$n_{2\omega}$	birefringent walkoff $\rho$ (degrees)
DBS GaAs	QPM $l_c = 106 \mu\text{m}$	61	0.01	52	3.271	3.296	0
DBS ZnSe	QPM $l_c = 112 \mu\text{m}$	37	0.0005	18	2.403	2.429	0
ZnGeP <sub>2</sub>	birefringent $\theta_{\text{pm}} = 90^\circ$ $T = 92^\circ\text{C}$	70	1	35	3.125	3.125	0
AgGaSe <sub>2</sub>	birefringent $\theta_{\text{pm}} = 55^\circ$	27	0.01	1	2.592	2.592	0.68

crystal	$dn/dT$ (°K <sup>-1</sup> )	$d\Delta n/dT$ (°K <sup>-1</sup> )	FOM <sub>cw</sub>	FOM <sub>p</sub>	FOM <sub>od</sub>	FOM <sub>hp</sub>
DBS GaAs	$149 \times 10^{-6}$	$1.6 \times 10^{-6}$	6,500	2.5	160	3,100
DBS ZnSe	$64 \times 10^{-6}$	$0.7 \times 10^{-6}$	2,400,000	2.4	2,400	33,000
ZnGeP <sub>2</sub>	(o) $150 \times 10^{-6}$ (e) $170 \times 10^{-6}$	$20 \times 10^{-6}$	1	3.8	(o)1.1 (e)1.0	2.4
AgGaSe <sub>2</sub>	(o) $70 \times 10^{-6}$ (e) $40 \times 10^{-6}$	$30 \times 10^{-6}$	2,600	1	(o)6.9 (e)12	1

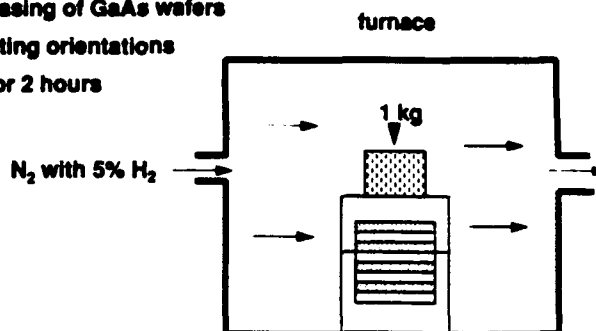
$d_{\text{eff}}$  effective nonlinear optical coefficient for birefringent phase matching  
 $d_{\text{Q}}$  effective nonlinear optical coefficient for quasi phase matching  
 $n_{\omega}$  index of refraction at 10.6  $\mu\text{m}$   
 $n_{2\omega}$  index of refraction at 5.3  $\mu\text{m}$   
 $dn/dT$  birefringent crystals have different derivatives for ordinary and extraordinary waves  
 $d\Delta n/dT$   $\Delta n = n_{2\omega} - n_{\omega}$

#### Normalized Figures of Merit

FOM<sub>cw</sub> Figure of merit for cw external resonant cavity SHG,  $\text{FOM}_{\text{cw}} = d_{\text{eff}}^2 / (n^3 \alpha^2)$   
FOM<sub>p</sub> Figure of merit for single-pass pulsed operation,  $\text{FOM}_{\text{p}} = d_{\text{eff}}^2 / n^3$   
FOM<sub>od</sub> Figure of merit for optical distortion,  $\text{FOM}_{\text{od}} = K / (\alpha dn/dT)$   
FOM<sub>hp</sub> Figure of merit for high average power,  $\text{FOM}_{\text{hp}} = d_{\text{eff}}^2 K / (\alpha n^2 d\Delta n/dT)$

## Wafer Preparation and Diffusion Bonding

- cut to 12 x 12 mm pieces
- standard degreasing of GaAs wafers
- stack in alternating orientations
- bake at 840 C for 2 hours



- bonded 2-9 layer stacks
- outer surfaces degraded during the processing
- need to be repolished for good optical quality

Fig. 3. Schematic drawing of the oven used for diffusion bonding. Steps of the bonding procedure are indicated

environment. Pressure was applied with a 1-kg weight, and the assembled stack was placed in an oven with a 5% H<sub>2</sub> and 95% N<sub>2</sub> atmosphere, ramped to 840° C over 1 hour, maintained for a two hour period, and cooled to room temperature over approximately 8 hours. A drawing of the oven is shown in Fig. 3.

Stacks with 2 through 9 layers were fused into monolithic units. We were able to bond layers regardless of their orientation, i.e. {110} to {110}, {100} to {100}, {100} to {110}, and the alignment was not critical. Observation with an IR microscope allowed imperfections in the bonding to be viewed. Some of our initial bonding attempts were marred by irregularities on the surfaces and by particles that became sandwiched between the layers. With successful bonding, the samples cleaved along the crystal planes leaving the bonded surfaces intact indicating the strength of the diffusion bond. The exterior surfaces of the stack, which were in contact with graphite spacers, were noticeably degraded. We did not repolish these surfaces as the resulting uncertainty in the layer thicknesses would have hampered analysis of the SHG results. Recently we have established the capability of polishing GaAs, and, in the future, we will cap the diffusion-bonded stacks with {100} layers, which have no effective nonlinear coefficient, and repolish the exterior surfaces prior to device testing.

### *B. Demonstration of phase-coherent SHG*

Second-harmonic generation was observed in five diffusion-bonded GaAs samples and compared to SHG in a single plate. Linearly polarized 10.6- $\mu\text{m}$  radiation, from a grating-tuned, Q-switched  $\text{CO}_2$  laser, was incident normal to the diffusion-bonded GaAs samples. Pulse durations of 200 ns with 2-MW/cm<sup>2</sup> peak intensity were used. Second-harmonic-output power at 5.3  $\mu\text{m}$  was measured with an InSb detector. The SHG power for normal incidence of the fundamental was measured as a function of the angle  $\Phi$  between the polarization of the fundamental and the  $\langle 110 \rangle$  direction for the purpose of characterizing the material and SHG process. The expected  $(1 + 3\sin^2\Phi)\cos^2\Phi$  dependence of the output power was observed. For the remainder of the measurements, the fundamental polarization was fixed along a  $\langle 111 \rangle$  direction.

Our wafers were not an odd multiple of  $l_c$  in thickness, and therefore, the conversion efficiency was not optimized for the 10.6- $\mu\text{m}$  fundamental wavelength. Maximum SHG conversion efficiency was observed with five plates. The measured thickness of the wafers was used to calculate the total phase mismatch as a function of the number of layers,  $N$ , and the output power was compared to the expected  $\sin^2(\Delta k_Q N l / 2)$  dependence, where  $l$  is the thickness of a single wafer. Figure 4 shows the experimental setup, and Fig. 5 shows relative SHG power for diffusion bonded stacks of 2, 3, 5, 7, and 9 layers, as well as for a single plate. The agreement with the expected dependence on the number of layers demonstrates the phase coherence of the diffusion-bonded GaAs stacks.

### *C. Preliminary Damage Measurements*

Many potential applications of these DB-QPM GaAs structures involve high average power. Therefore, some preliminary damage measurements were performed. Both a bulk GaAs and a diffusion-bonded GaAs sample were placed in a 26-W cw  $\text{CO}_2$  laser beam which was focused to a 60- $\mu\text{m}$   $1/e^2$ -peak-intensity radius, producing an intensity of 0.5MW/cm<sup>2</sup>. No damage was detected. A 1-kHz pulsed  $\text{CO}_2$  laser with 60- to 500- $\mu\text{s}$  pulse width was focused to a peak intensity of 30 MW/cm<sup>2</sup>. No damage was seen in the bulk GaAs. We were unable to obtain accurate data for the diffusion-bonded GaAs stacks at this power level because the degraded outer surfaces developed damage characteristic of thermal runaway; however, the samples were not noticeably damaged with a single pulse. Additional damage measurements will be conducted with repolished exterior surfaces in the near future.

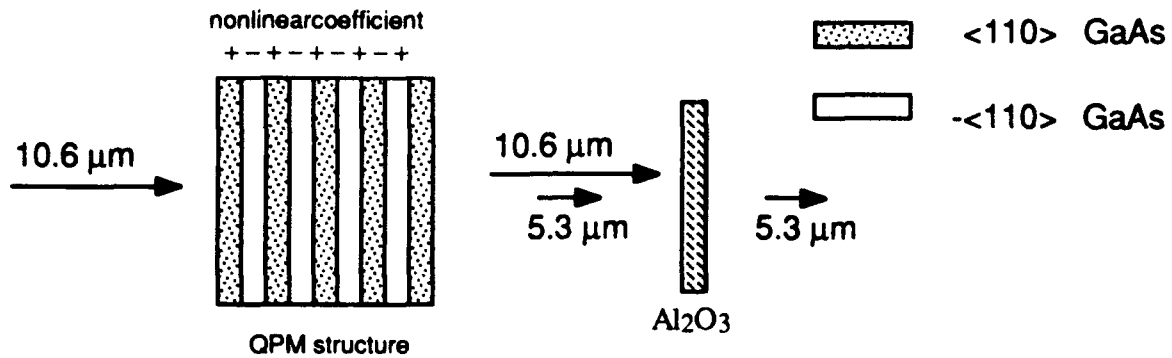


Fig. 4. Schematic drawing of experimental setup for SHG

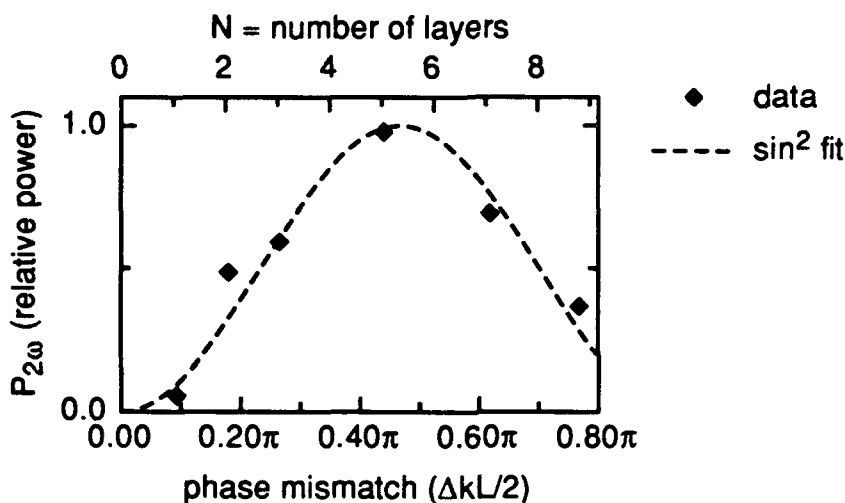


Fig. 5. The sine squared dependence of the SHG signal shows the phase coherence of the SHG process in the diffusion-bonded stack of GaAs wafers.

#### D. Coherence length and tolerance calculations

Coherence length calculations for nonlinear interactions that are of interest are useful to show the potential performance of diffusion-bonded structures. Coherence lengths for SHG have been presented in Fig. 2. Here coherence lengths for the 3-wave processes optical parametric oscillation (OPO) and difference frequency generation are presented.

An OPO pumped at the frequency  $\omega_p$  generates two lower frequencies, the signal and idler, at  $\omega_s$  and  $\omega_i$ . Conservation of energy requires that the frequencies of the signal and idler sum to the frequency of the pump. For the OPO coherence length calculations described here, it was assumed that the pump was at 2.128  $\mu\text{m}$ . This is the output wavelength of a degenerate OPO pumped with a 1.064- $\mu\text{m}$  Nd:YAG laser. Such an OPO

can be constructed from KTP or LiNbO<sub>3</sub> for example. The tuning curves are presented as a function of the coherence length, which is double valued in wavelength. The two wavelengths are those of the signal and idler for which quasi phase matching occurs. The OPO tuning curves are shown in Figs. 6 and 7. A remarkable property of these curves is the small change in coherence length for relatively large changes in signal and idler wavelength. This indicates a large spectral acceptance, which could be useful for optical parametric amplification and sum frequency generation or infrared up conversion applications.

For difference frequency generation it was again assumed that the incident radiation was generated by an OPO pumped at 1.064 μm. In this case, however, the 1.064-μm-pumped OPO is not at degeneracy. The generated OPO signal and idler frequencies are mixed in the diffusion-bonded stack. The difference frequency wavelengths for GaAs and ZnSe are shown in Figs. 8 and 9.

The calculation of tolerances on wafer thickness are also important to the fabrication process and closely related to the coherence length calculations. The tolerance for QPM interactions were derived by Fejer *et al.* [4]. The largest constant error of the thickness of individual layers that can be tolerated and have the small depletion nonlinear conversion at 50% of its maximum value is

$$\delta l = \pm 0.87 l_c / N,$$

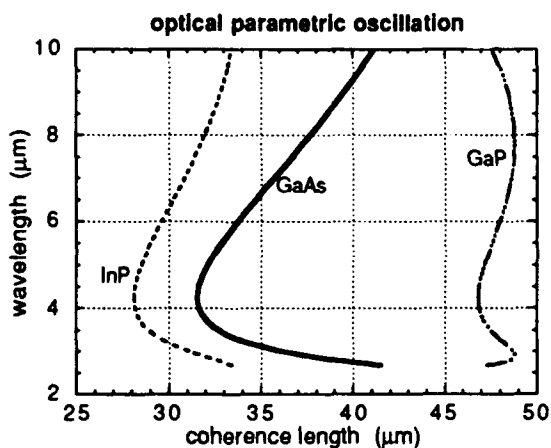


Fig. 6. Parametric oscillator tuning curves for III-V semiconductor compounds for a 2.13-μm pump wavelength. The dispersion of GaP allows very wide wavelength tuning at a fixed coherence length of 48 μm.

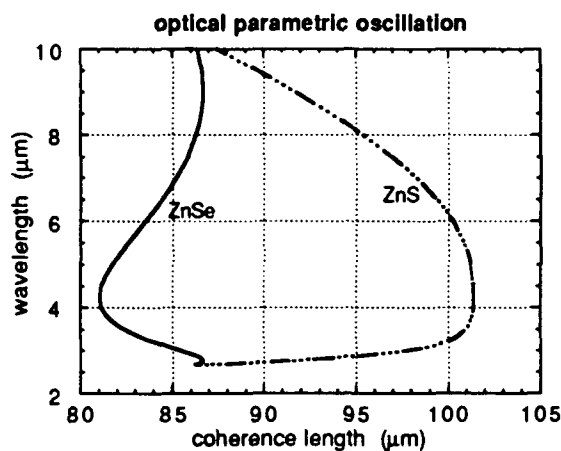


Fig. 7. Parametric oscillator tuning curves for II-VI compound ZnSe and ZnS. The low absorption loss of ZnSe may allow very high average power parametric oscillator devices when pumped at 2.13 μm. For ZnS tuning over the 3- to 6-μm band is possible for a fixed layer thickness of 101 μm.

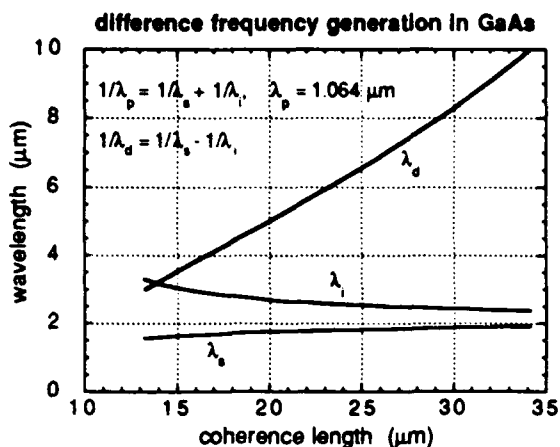


Fig. 8. Difference frequency generation in diffusion-bonded GaAs for mixing the signal and idler from a 1.06- $\mu\text{m}$ -pumped OPO. The output difference frequency  $\lambda_d$  vs. the coherence length is shown.

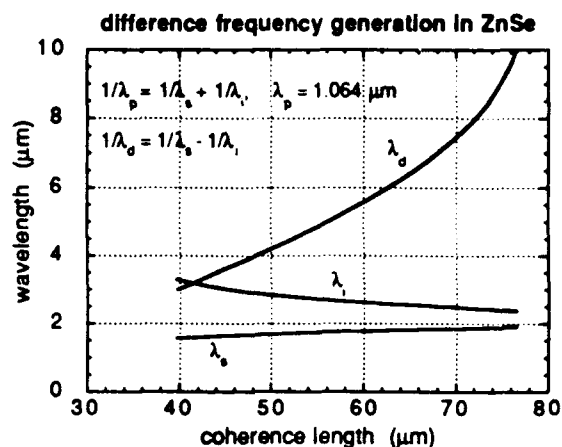


Fig. 9. Difference frequency generation  $\lambda_d$  for ZnSe when pumped by the signal and idler from a 1.06- $\mu\text{m}$ -pumped OPO. Here the coherence length is substantially larger than for GaAs.

where  $l_c$  is the coherence length for the process and  $N$  is the number of layers. Note that the result as stated here is independent of the QPM order. For a 1-cm-long 94-layer diffusion-bonded GaAs stack used for SHG of a 10.6- $\mu\text{m}$  CO<sub>2</sub> laser, the largest constant thickness error is  $\pm 1 \mu\text{m}$ .

Random thickness errors are described by the standard deviation of a normal distribution of thickness errors that would reduce conversion to 50% of its maximum value

$$\sigma_l = 0.87l_c / \sqrt{N}.$$

For the same 94-layer stack, the maximum standard deviation is  $\sigma_l = 9.5 \mu\text{m}$ .

Spectral, angular, and temperature acceptances are given in Table III. Acceptances for QPM SHG in diffusion-bonded-stacked (DBS) GaAs and ZnSe are compared those for birefringently phase matched AgGaSe<sub>2</sub> and ZnGeP<sub>2</sub>. For the example of 1-cm GaAs stack, the acceptance angle FWHM is 64° for SHG of CO<sub>2</sub> laser output. The spectral acceptance for changes in the pump wavelength is 0.5  $\mu\text{m}$ , and the acceptance temperature is 270°C. These acceptance values are more than one order of magnitude greater than for birefringent phase matched crystals.

It is important to understand the range of conditions over which various conversion efficiency approximations are valid. We begin by asking when is it accurate to use the SHG conversion relationships obtained for conventional phase matching for quasi-phase-matched SHG with the QPM effective nonlinear coefficient? The conversion efficiencies

TABLE III. Comparison of Acceptances for SHG in ZnGeP<sub>2</sub> and AgGaSe<sub>2</sub> and Diffusion-Bonded-Stacked (DBS) GaAs and ZnSe for 1-cm-long crystals.

crystal	$\Delta\lambda$ ( $\mu\text{m}$ )	$\Delta\theta_{\text{ext}}$ (degrees)	$\Delta T$ ( $^{\circ}\text{K}$ )
DBS GaAs	0.48	64	270
DBS ZnSe	0.2	38	<500
ZnGeP <sub>2</sub>	0.06	41	16
AgGaSe <sub>2</sub>	0.12	2	16

Full widths at half maximum are shown for fundamental wavelength, external angle, and temperature acceptances.

predicted by three different monochromatic planewave approximations for SHG in a diffusion-bonded GaAs stack of plates are shown in Fig. 10. A fundamental input intensity of 300 MW/cm<sup>2</sup> was assumed for these calculations. The small depletion approximation is valid for conversion efficiency up to approximately 20%, which occurs at the 10th plate in the stack. The hyperbolic tangent solution, which applies to perfect phase matching with an effective nonlinearity appropriate for quasi phase matching,  $d_Q$ , agrees with the exact elliptic function solution for up to 100 layers and nearly 100% conversion. The tanh solution, however, does not allow for small changes in the coherence length that cause the conversion to reverse after 150 layers. The conclusion illustrated here is that the QPM nonlinear frequency conversion process in the layered material can be treated as a process in a homogeneous material up to a point, but inaccuracy develops for under conditions that would result in very high conversion in the homogeneous material. Such conditions can be reached at the peak of a pulse when an attempt is made to achieve high conversion efficiency in the lower intensity temporal or spatial wings.

#### E. Calculations of frequency conversion

We now provide calculations for the efficiency of QPM nonlinear frequency conversion in DBS materials. The approach is to estimate conversion efficiency starting with a monochromatic planewave approximation and then build to more complex approximations. The monochromatic planewave approximation assumes uniform temporal and spatial distributions. This simplicity allows us to more easily investigate some issues

such as saturation and the validity of certain approximations. The assumption of uniformity, however, limits applicability to "top-hat" distributions or small regions of actual pulses and beams that can be treated as uniform distributions and have insignificant divergence and walkoff. Simple techniques of averaging monochromatic planewave solutions can be used for many of the spatial distributions of weakly focused beams and temporal pulse shapes with no short duration structure. More tightly focused beams require the consideration of diffraction. Extremely short temporal structure would require consideration of group velocity walkoff effects. Calculations are presented for SHG and difference frequency generation (DFG) conversion efficiency and optical parametric oscillator (OPO) thresholds.

It is shown in Fig. 10 that only 50 layers are needed for single pass SHG conversion efficiency of 80% with an incident intensity of  $300 \text{ W/cm}^2$  on the DBS GaAs. We observed that the damage threshold for our preliminary DBS GaAs samples was at least

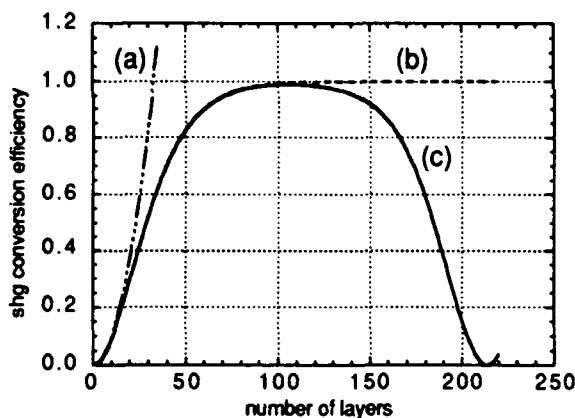


Fig. 10. Three monochromatic planewave solutions are compared for SHG in QPM GaAs stack of plates. (a) Small depletion approximation, (b) perfectly phase-matched large-depletion approximation, and (c) exact elliptic function solution that considers non-zero phase-mismatch in each plate of the QPM stack and the sign change of the nonlinear coefficient in each successive plate. The fundamental intensity is  $300 \text{ MW/cm}^2$ . The layers are assumed to be exactly one coherence length thick for 10.6- to 5.3- $\mu\text{m}$  SHG.

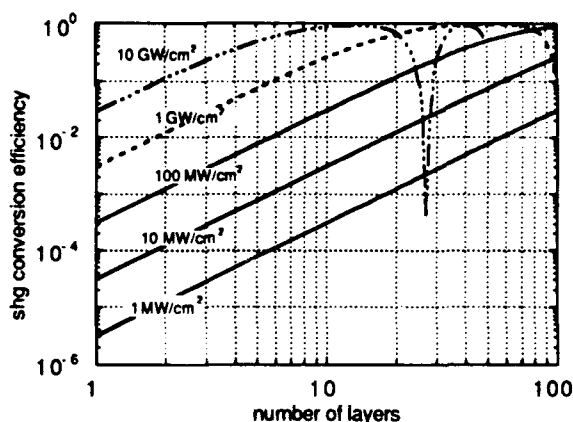


Fig. 11. Exact elliptic function solution for 10.6- to 5.3- $\mu\text{m}$  SHG in a QPM stack of GaAs plates each exactly one coherence length thick. Conversion efficiency is shown as a function of the number of layers for different intensities as indicated.

300 W/cm<sup>2</sup> for Q-switched CO<sub>2</sub> laser output. Other intensities are of interest for laser outputs with different durations. Figure 11 shows the exact elliptic function solution for monochromatic plane wave SHG as a function of the number of layers in a diffusion-bonded GaAs structure for different intensities. The elliptic function solutions treat harmonic generation in each layer individually and allow for fundamental depletion, phase changes at high levels of conversion, and changes in the coherence length. The range of intensities is typical of those that would be encountered for SHG conditions varying from low-power cw resonant cavity conditions to high peak power single pass mode-locked pulses. The monochromatic planewave solutions are applicable to intensity distributions uniform in time and space..

Two example calculations are presented for SHG in diffusion-bonded GaAs pumped by 10.6-μm laser radiation. These examples are typical of laboratory demonstrations that will be attempted. First, Example 1 shows that 45% SHG total conversion should be achieved in a 50-layer structure when pumped by a 10.6-μm pulse of 300-MW/cm<sup>2</sup> peak intensity. The conversion efficiency given in this example is total conversion for a pulse that is Gaussian in time and space. The conversion efficiency of 83% at 50 layers shown

#### Example calculation 1. Single-pass pulsed SHG in DB-QPM GaAs

GaAs, 50 layers, 1st order,  $l_c = 106 \mu\text{m}$   
 $\lambda_\omega = 10.6 \mu\text{m}$ ,  $\lambda_{2\omega} = 5.3 \mu\text{m}$ ,  $n_\omega = 3.27$   $n_{2\omega} = 3.30$   
 Assume fundamental pulse Gaussian in time and space  
 $I_\omega(r,t) = I_{\omega,0} \exp(-2r^2/w_0^2) \exp(-2t^2/\tau^2)$

pump beam spot size:	$w_0 = 1 \text{ mm}$
pump pulse $1/e^2$ intensity halfwidth:	$\tau = 30 \text{ ns}$
crystal length:	$l = 5.31 \text{ mm}$
incident peak pump intensity:	$I_{\omega,0} = 300 \text{ MW/cm}^2$
incident pump energy:	$W_\omega(0) = 177 \text{ mJ}$
effective QPM nonlinear coefficient:	$d_Q = 61 \text{ pm/V}$



Conversion efficiency calculations

$$\text{small-depletion, near-field approximation: } \eta_0 = \frac{W_{2\omega}(l)}{W_\omega(0)} = \frac{1}{2\sqrt{2}} \Gamma_0^2 l^2,$$

$$\text{where } \Gamma_0^2 = \frac{2\omega^2 d_Q^2}{n_{2\omega} n_\omega^2 c^3 \epsilon_0} I_{\omega,0} \text{ and } \omega = 2\pi c/\lambda_\omega = 1.78 \times 10^{14} \text{ s}^{-1}.$$

correction for arbitrary values of fundamental depletion:  $\eta_d = \eta_0/(1 + \eta_0)$   
 estimated conversion efficiency with depletion: 45%

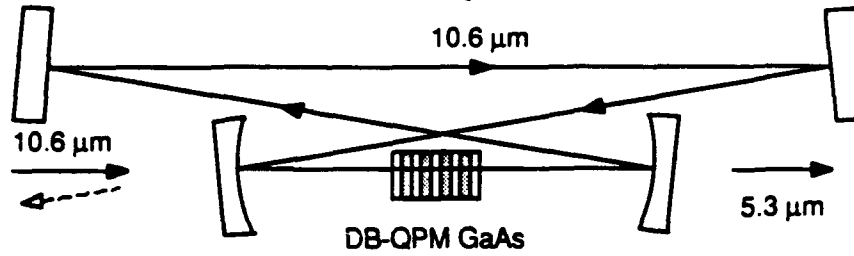
in Fig. 10 is the monochromatic planewave result and closely approximates the conversion expected at the peak of the pulse. The result of Example 1 is applicable to a high-peak-power single-pass SHG experiment.

Example 2 shows that high efficiency SHG is possible in an external resonant cavity. Here it is assumed that losses from imperfect reflection at the cavity mirrors and unwanted reflection at the crystal surfaces are 2% per cavity transit. For a incident cw 10.6- $\mu\text{m}$  beam of 10 watts power, 2.4 watts of 5.3- $\mu\text{m}$  radiation is generated for a sample of 50 layers. If the cavity losses were reduced from 2% to 1%, conversion efficiency would nearly double. Both of these harmonic generators would be practical useful devices. Our preliminary experimental observations also indicate this type of performance should be possible.

**Example calculation 2. Externally resonant cw SHG in DB-QPM GaAs**

GaAs, 50 layers, 1st order,  $l_c = 106 \mu\text{m}$   
 $\lambda_\omega = 10.6 \mu\text{m}$ ,  $\lambda_{2\omega} = 5.3 \mu\text{m}$ ,  $n_\omega = 3.27$   $n_{2\omega} = 3.30$

pump beam spot size:  $w_0 = 100 \mu\text{m}$   
 crystal length:  $l = 5.31 \text{ mm}$   
 Boyd and Kleinman focusing parameter:  $\xi = 0.273$   
 Boyd and Kleinman focusing factor:  $h_m(B=0, \xi) = 0.267$   
 incident pump power:  $P_1 = 10 \text{ W}$   
 cavity reflectivity product:  $R_2 = 0.98$   
 intensity absorption coefficient:  $\alpha = 0.008 \text{ cm}^{-1}$   
 single pass crystal transmission:  $T = \exp(-\alpha l) = 0.996$   
 effective QPM nonlinear coefficient:  $d_Q = 61 \text{ pm/V}$



Conversion efficiency calculations

Harmonic generation coefficient: 
$$\gamma_{SH} = \frac{\xi}{h_m(B, \xi)} \frac{\omega^2 d_Q^2}{n_\omega^2 n_{2\omega} \epsilon_0 c^3} \frac{l^2}{\pi w_0^2 / 2} = 2.44 \times 10^{-5} \text{ W}^{-1}$$

Impedance matched mirror reflectivity:

$$R_m = \frac{1 + TR_2 - \sqrt{(1 + TR_2)^2 - 4TR_2(1 - \gamma_{SH} P_1)}}{2} = 0.9684$$

Circulating fundamental power inside cavity:  $P_c = P_1 / (1 - R_m) = 316 \text{ W}$

Peak circulating fundamental intensity:  $I_{c,0} = P_c / (0.5 \pi w_0^2) = 2.01 \text{ MW/cm}^2$

Harmonic power:  $P_{SH} = \gamma_{SH} P_c^2 = 2.44 \text{ W}$

Conversion efficiency:  $\eta = P_{SH} / P_1 = 24\%$

Figure 12 shows the monochromatic planewave solutions for difference frequency generation (DFG). The small signal solution assumes that there is no depletion of the two waves incident on the diffusion-bonded GaAs crystal stack. The general monochromatic planewave solution allows changes of the two incident waves with propagation through the nonlinear material and shows the oscillatory nature of DFG. When the pump wave at  $1.71 \mu\text{m}$  is completely depleted, the conversion process must reverse. Figure 13 shows the general solution for DFG in a GaAs structure as a function of the number of layers for different intensities. These solutions describe DFG for input intensities that are uniform in space and time. If diffraction and walkoff are not of concern, the monochromatic planewave solutions can be averaged over the input intensity distributions to obtain total conversion using techniques similar to those used for SHG of beams or pulses.

Optical parametric oscillation is addressed in Examples 3 - 5. In a singly resonant OPO (SRO) only one of the waves, signal or idler, is resonant. The other wave is assumed to build up from zero intensity on each cavity transit. In a doubly resonant OPO (DRO) both signal and idler are resonant. The parametric oscillation builds up from the initial radiation that is in the cavity when pumping begins. The initial radiation can be either

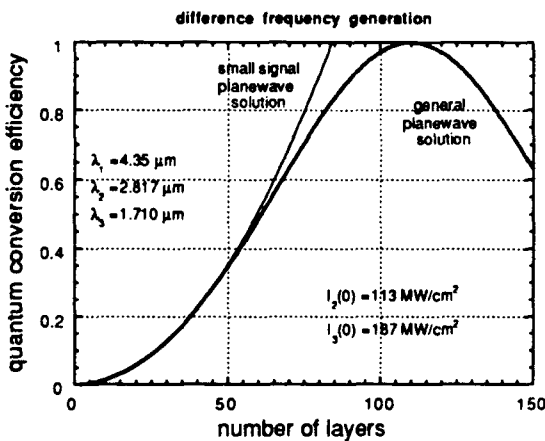


Fig. 12. Monochromatic planewave solutions are compared for DFG in a QPM stack of GaAs plates. The small signal solutions treats the incident waves as constant during propagation through the nonlinear material. The general solution considers wavevector mismatch in each layer, reversal of the nonlinear coefficient, and changes in amplitude and phase of all waves. The small signal solution does not show the oscillatory nature of DFG.

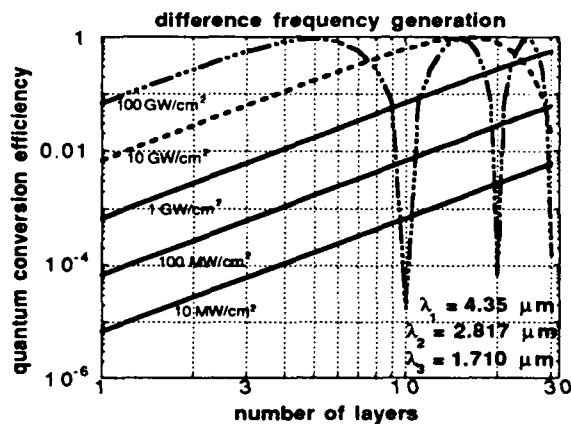


Fig. 13. Exact elliptic function solution for DFG in a QPM stack of GaAs plates each exactly one coherence length thick. Conversion efficiency is shown as a function of the number of layers for different intensities as indicated.

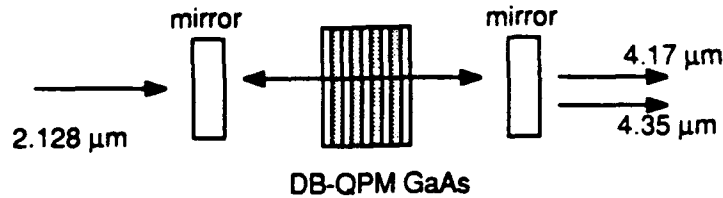
quantum zero point fluctuations or a higher intensity injected from an external source. Threshold for a cw OPO is defined as the pumping level at which the low level gain exceeds cavity losses. In a pulsed OPO is it necessary not only for gain to exceed losses, but the oscillation must build up to an observable level in the duration of the pump pulse.

In examples 3 and 4, two materials are compared for SRO operation, GaAs and ZnSe. For both cases the pump wavelength is 2.128  $\mu\text{m}$ . A third order QPM stack with 95.7- $\mu\text{m}$  layer thickness is used for GaAs because of the short (32  $\mu\text{m}$ ) coherence length, whereas a first order QPM stack is used for ZnSe with the longer (82  $\mu\text{m}$ ) coherence length. SRO thresholds are calculated using the analysis of Brosnan and Byer [17] with one modification. The inverse hyperbolic cosine is evaluated exactly avoiding the approximation of large gain. The assumed pump beam spot size of 1 mm is large enough

### Example calculation 3. Pulsed DB-QPM GaAs SRO

GaAs, 100 layers, 3rd order,  $3l_c = 95.7 \mu\text{m}$   
 $\lambda_p = 2.128 \mu\text{m}$ ,  $\lambda_s = 4.17 \mu\text{m}$ ,  $\lambda_i = 4.35 \mu\text{m}$ ,  $n_p = 3.34$   $n_s = 3.30$   $n_i = 3.30$   
 Assume pump pulse Gaussian in time and space  
 $I_p(r,t) = I_{p,0} \exp(-2r^2/w_p^2) \exp(-2t^2/\tau^2)$

pump beam spot size:	$w_p = 1 \text{ mm}$
pump pulse $1/e^2$ intensity halfwidth:	$\tau = 10 \text{ ns}$
crystal length:	$l = 9.57 \text{ mm}$
physical cavity length:	$L' = 2.0 \text{ cm}$
mirror curvature:	flat
spatial mode coupling coefficient:	$g_s = 0.807$
absorption coefficient:	$\alpha = .01 \text{ cm}^{-1}$
cavity reflectivity product:	$R = 0.8$
effective QPM nonlinear coefficient:	$d_Q = 20 \text{ pm/V}$



Threshold calculations

$$\cosh(\bar{\Gamma}l) = \exp\left\{2\alpha l - \frac{1}{2} \ln R + \frac{L}{2\tau c} \ln\left(\frac{P_{\text{thres}}}{P_0}\right)\right\}$$

$$\text{using } \ln\left(\frac{P_{\text{thres}}}{P_0}\right) = 33, \quad \kappa = \frac{2\omega_s\omega_i d_Q^2}{n_s n_i n_p \epsilon_0 c^3} \quad \text{and } L = L' + (n_s - 1)l$$

$$\text{peak energy fluence} = J_0 = \frac{2.25\tau}{\kappa g_s l^2} (\bar{\Gamma}l)^2 = 1.37 \text{ J/cm}^2$$

$$\text{peak intensity} = I_0 = 110 \text{ MW/cm}^2$$

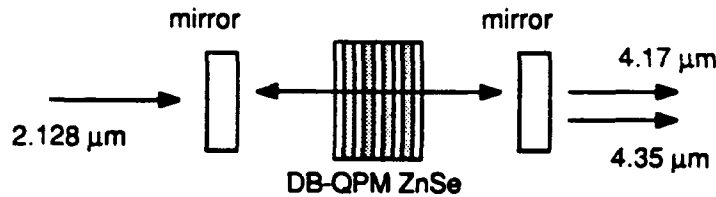
$$\text{total pulse energy} = W = 22 \text{ mJ.}$$

that the mode coupling coefficient remains close to unity for both cases, i.e. diffraction does not cause a significant increase in threshold. In both cases the number of layers of the DBS structures is chosen to give an threshold pump energy of approximately 20 mJ and a peak pump intensity at threshold near 100 MW/cm<sup>2</sup>. These calculated results are for typical conditions. Threshold powers could be adjusted upward or downward by changing the pump beam size and adjusting cavity geometry. Reasonable OPO conversion efficiency is obtained pumping at a level a few times above threshold. Calculation for both the diffusion-bonded GaAs and ZnSe QPM SRO's show these devices are practical for laboratory implementation. The ZnSe device is particularly attractive because of the longer coherence length and smaller required number of layers.

**Example calculation 4. pulsed DB-QPM ZnSe SRO**

ZnSe, 30 layers, 1st order,  $l_c = 82 \mu\text{m}$   
 $\lambda_p = 2.128 \mu\text{m}$ ,  $\lambda_s = 4.17 \mu\text{m}$ ,  $\lambda_i = 4.35 \mu\text{m}$ ,  $n_p = 2.43$ ,  $n_s = 2.42$   $n_i = 2.42$

pump beam spot size:	$w_p = 1 \text{ mm}$
pump pulse $1/e^2$ intensity halfwidth:	$\tau = 10 \text{ ns}$
crystal length:	$l = 2.45 \text{ mm}$
physical cavity length:	$L' = 2.0 \text{ cm}$
mirror curvature:	flat
spatial mode coupling coefficient:	$g_s = 0.871$
absorption coefficient:	$\alpha = 0.5 \text{ m}^{-1}$
cavity reflectivity product:	$R = 0.8$
effective QPM nonlinear coefficient:	$d_Q = 36.8 \text{ pm/V}$



**Threshold calculations**

$$\cosh(\bar{\Gamma}l) = \exp\left\{2\alpha l - \frac{1}{2} \ln R + \frac{L}{2\tau c} \ln\left(\frac{P_{\text{thres}}}{P_0}\right)\right\}$$

using  $\ln\left(\frac{P_{\text{thres}}}{P_0}\right) = 33$ ,  $\kappa = \frac{2\omega_s\omega_i d_Q^2}{n_s n_i n_p \epsilon_0 c^3}$  and  $L = L' + (n_s - 1)l$

$$\text{peak energy fluence} = J_0 = \frac{2.25\tau}{\kappa g_s l^2} (\bar{\Gamma}l)^2 = 1.5 \text{ J/cm}^2$$

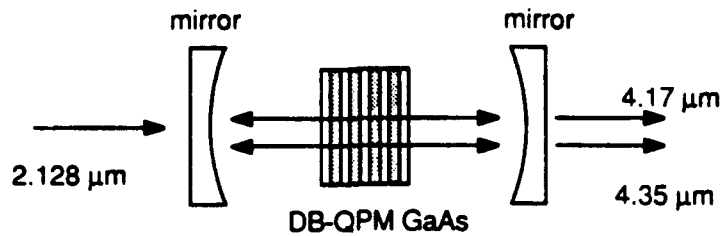
$$\text{peak intensity} = I_0 = 116 \text{ MW/cm}^2$$

$$\text{total pulse energy} = W = 23 \text{ mJ.}$$

**Example calculation 5. DB-QPM GaAs cw DRO**

GaAs, 100 layers, 3rd order,  $3l_c = 95.7 \mu\text{m}$   
 $\lambda_p = 2.128 \mu\text{m}$ ,  $\lambda_s = 4.17 \mu\text{m}$ ,  $\lambda_i = 4.35 \mu\text{m}$ ,  $n_p = 3.34$   $n_s = 3.30$   $n_i = 3.30$

crystal length:  $l = 9.57 \text{ mm}$   
 assume round trip amplitude losses:  $a_s = a_i = 0.01$   
 mirror curvature: to give  $\bar{h}_m(B=0, \xi = 1.19) = 0.854$   
 effective QPM nonlinear coefficient:  $d_Q = 20 \text{ pm/V}$



Threshold calculations

$$P = \frac{\pi}{l \bar{h}_m(B, \xi)} \frac{a_s a_i n_s n_i c^4 \epsilon_0}{\omega_p \omega_s \omega_i d_Q^2} = 0.43 \text{ W}$$

$$\xi = l / (w_0^2 k) = 1.19 \text{ requires a spot size of } w_0 = 29 \mu\text{m}$$

The maximum pump intensity at threshold is  $I_0 = 34 \text{ kW/cm}^2$

A DRO is considered in Example 5. For this example mild focusing to a small spot size is used. The DRO threshold is calculated using the theory of Boyd and Kleinman [18]. The calculation again is for a 2.128- $\mu\text{m}$  pump, but in this case a cw pump is used. Cavity-round-trip amplitude losses of 1% corresponding to 2% intensity losses are used. The same 100-layer, 3rd-order DB-QPM GaAs structure used in Example 3 is used here. The threshold pump power is 0.43 watts with a reasonable peak intensity at threshold of 34  $\text{kW/cm}^2$ . This is not an unreasonable pump required for either a cw 1.064- $\mu\text{m}$ -pumped OPO or a cw Ho or Tm laser. Diode-laser-pumped Ho and Tm lasers have operated at 15 W cw output power.

The preliminary research discussed here along with the projection calculations of device performance are very encouraging. We are now prepared to accelerate our research effort in several areas. It is necessary to develop an in-depth understanding of the diffusion bond process to proceed with the construction and testing of the nonlinear infrared devices now that the preliminary investigations have shown that diffusion bonding of up to 9 layers is possible.

#### IV. Future Research

The goal of this investigation is to demonstrate practical devices for nonlinear mid-IR frequency conversion with diffusion-bonded-stacked (DBS) GaAs. The cycle of sample preparation, material characterization, and device testing is the essence of this program. We will use device performance as the ultimate test of the diffusion-bonding approach for infrared generation. Diffusion-bonded-stacked (DBS) GaAs quasi-phase-matched (QPM) optical parametric oscillators (OPO's) pumped at 2  $\mu\text{m}$  are of primary interest in this research. We will also continue to study harmonic generation pumped by CO<sub>2</sub> laser output because it is important for materials characterization and fixed wavelength mid-IR generation. Difference-frequency-generation (DFG) pumped by the dual-wavelength output of 1- $\mu\text{m}$ -pumped OPO's and optical parametric generators (OPG's) will also be investigated in DBS materials. Material processing studies will build on the preliminary results described here. We will be coordinating with 2- $\mu\text{m}$  source development at NRaD and Lightwave Electronics to use their sources for device testing at 2  $\mu\text{m}$ . Damage testing will continue in collaborative studies with companies such as Coherent. We have also received inquiries from a number of companies that are interested in the DBS materials development. In parallel work, we will begin diffusion bonding studies in other III-V and II-VI semiconductors as good crystal quality becomes available.

##### *A. Material Processing Studies*

Before fabricating the devices, it is necessary to understand and be able to predict the bonding mechanisms. Once the mechanisms are understood the processing will need to be extended to large numbers of layers. We expect three aspects of the processing to potentially limit the size of the devices. Firstly, as the number of layers increase, the tolerances on the thickness and parallelism of the wafers will also increase. We have recently purchased a lapping and polishing machine, which should allow us to meet the tolerances required for a 100-layer structure for SHG of CO<sub>2</sub> radiation. Secondly, minute losses due to bonding imperfections in a 10-layer structure could become important for a 100 layer structure; therefore, it is important to develop the best diffusion bonding techniques possible. Thirdly, the bonding parameters: temperature, pressure, and time, might need to be varied to accommodate the additional layers.

An understanding of the bonding mechanisms in GaAs will aid studies of bonding mechanisms in other semiconductors. Hopefully, most of what has been learned for GaAs will transfer directly to other semiconductors. We expect optimization of the bonding parameters will depend on the relative melting temperatures, mass transfer characteristics and mobilities. ZnSe is interesting because it is transparent into the visible, and has an

extremely low absorption coefficient throughout the mid-IR. It is potentially better than GaAs for very high power applications; however, it has not been possible to grow large single crystals of ZnSe until the last couple of years, and the growth techniques and crystal quality are not as well understood or advanced as those of GaAs. As growth techniques improve for the zinc-blende semiconductors, we will expand the program to encompass the most interesting prospects.

### *B. Characterization*

Accurate knowledge of bulk material parameters is required for device design, and intensive characterization will need to be done because of the large uncertainties that exist in the available data. Device characterization is necessary for comparison with the bulk parameters, and evaluation of the diffusion-bonding process. The uncertainty in available data is demonstrated by the range of values that exists for nonlinear coefficients of the II-VI and III-V materials. Differences of factors of two and three are common in tabulations of nonlinear coefficients. Our investigations will include direct nonlinear coefficient measurements and measurements inferred from device performance.

Infrared absorption in these materials is another critical issue. It is possible that the diffusion bonding process will alter absorption properties. Therefore we will be making absorption, scattering and total transmission measurements on the DBS GaAs and compare the results to similar measurements on bulk material. We will make laser calorimetric measurements of absorption, measure scattering with a scatterometer, and compare the results with transmission measurements. These measurements will be coordinated with material processing studies and device development for optimization of device performance. Our existing facilities will permit us to measure transmission continuously in the region of interest from 1 to 10  $\mu\text{m}$ . Scattering and absorption can be measured at the wavelengths of any available lasers. Initially we will be measuring these parameters at 10, 2, and 1  $\mu\text{m}$ .

Since many potential applications of DBS GaAs involve high peak power, and high average power conversion, we will continue damage measurements of the devices. We will perform the measurements at 1, 2 and 10- $\mu\text{m}$  looking for both single-shot and average-power damage thresholds. Lightwave Electronics, Coherent Inc. and other companies have volunteered high power lasers to help us make some of the damage measurements. We will also be developing appropriate mounts that will permit cooling of the devices to allow testing to high average power levels.

Some characterization will be required to maintain manufacturing tolerances, such as interferometric measurement wafer thickness and uniformity. Interferometry and infrared

microscopy will be used to measure surface quality of individual wafers and the optical quality of DBS GaAs.

When we are able to successfully diffusion bond other semiconductors, we will expand the characterization program to encompass the new materials. At this later stage of the program, we will be able to select more optimal materials for specific applications.

### *C. Theory*

We have already completed some initial calculations of device design and performance. As we better understand the material processes, and measure the bulk material parameters, we will be able to improve the theoretical predictions for the different configurations. We plan to calculate theoretical losses, thresholds and conversion efficiencies before fabricating any devices.

### *D. Devices*

Device development is planned in a number of steps. With each new device, we will first demonstrate the proof of principle, followed by improved designs and configurations to increase the conversion efficiency. Initial device characterization will be performed by SHG pumped with CO<sub>2</sub> laser radiation. The simplicity of SHG lends itself to the characterization of the linear and the nonlinear optical properties of the DBS GaAs devices, while, at the same time, generation of harmonic CO<sub>2</sub> laser radiation will be a very useful source of 5.3- $\mu$ m radiation.

We first plan to fabricate single pass SHG devices using different pulsed CO<sub>2</sub> lasers. This will confirm the capability of the material for high conversion efficiency at a low-average-output power. We also plan to test DBS GaAs for cw SHG using externally resonant SHG. This experiment will test the ability to construct low-loss stacks of diffusion bonded GaAs with a minimum of 50 layers. In related cw SHG work, we plan to investigate the potential for SHG, third-harmonic generation (THG) and fourth-harmonic generation (FHG) in the same external resonant cavity. This can be achieved by creating a diffusion-bonded stack that includes coherence lengths for SHG and for THG. Layers at the coherence length for FHG can also be bonded to the stack. Additionally, the coherence length for the generation of the fifth harmonic near 2  $\mu$ m is very close to the coherence length for SHG of the CO<sub>2</sub> laser: therefore, we expect the higher harmonic to be present as well. One application of this resonant SHG process is the generation of high average power at the third harmonic for coherent laser radar applications. A second application of this source is for absolute frequency references across the infrared to the 2- $\mu$ m and even the 1- $\mu$ m spectral region. For example, the CO<sub>2</sub> laser can have an absolute frequency stability of near 10 Hz when locked to OsO<sub>4</sub>. If this laser could be frequency converted and phase

locked to the 1064- $\mu\text{m}$  Nd:YAG laser then the absolute frequency stability of 1000 Hz at the Nd:YAG frequency could be realized. This is fully three orders of magnitude improvement in absolute frequency at the Nd:YAG wavelength compared to the presently known frequencies.

A primary goal of the proposed research is to develop DBS-GaAs 2- $\mu\text{m}$ -pumped QPM OPO's. This will be the first demonstrated IR quasi-phase-matched OPO. Initial OPO demonstrations will be at a fixed wavelength. They will be tested using both the NRaD 2- $\mu\text{m}$  source which is currently being developed and the diode-pumped Q-switched Tm:YAG laser manufactured by Lightwave Electronics. The available intensities from these sources should be adequate to obtain SRO operation for DBS GaAs with 50 layers. We propose to build both DRO and SRO OPO's from the DBS material. Initially, the OPO's will be third-order quasi phase matched. This will simplify the wafer thinning and handling.

Later in the program we propose to investigate wedged DBS structures that will allow QPM wavelength tuning by lateral translation. For example, a GaAs wafer could be wedged from 70 - 120  $\mu\text{m}$ , which is a wedge of 30 arc seconds for a 6-cm length. These pieces could be assembled within a pair of oppositely wedged end caps to provide a straight optical path. This would provide a third order QPM continuously tunable 2- $\mu\text{m}$ -pumped OPO. The first DBS QPM OPO's fabricated will use external mirrors to form the resonating cavity. In later experiments, we plan to build monolithic OPO's using the coated or uncoated surfaces of the devices. Further, with appropriate wedging of the end caps, the axial mode of the OPO cavity can also be tuned such that single-mode operation could be maintained over an extended wavelength range.

As an alternative approach for producing wavelengths in the 3 to 5- $\mu\text{m}$  region, we plan to build single-pass difference-frequency generators. Initially, we plan to fabricate fixed wavelength DFG's for existing lasers. In the later part of the program, we plan to develop a laser system to demonstrate high conversion efficiency DFG's. We propose to construct a Q-switched, injection-seeded, mode-locked Nd:YAG laser. This would be used to pump an OPO/OPA. Crystals being investigated for the OPO/OPA are KTP, LiNbO<sub>3</sub>, and periodically poled LiNbO<sub>3</sub> (PPLN). PPLN has the potential of much higher conversion efficiency because the nonlinear coefficient for the QPM interaction,  $d_{33}$ , is one order of magnitude larger than the effective nonlinear coefficient for the bulk interaction in LiNbO<sub>3</sub>. PPLN is being developed in our laboratory as an alternative crystal for visible and near-infrared nonlinear frequency conversion. The signal and the idler from the OPO/OPA will then be passed through a DBS GaAs DFG to obtain the difference

frequency. The mode-locked 10- to 100-ps pulses should provide the high intensities necessary to move the DBS GaAs DFG into the high conversion efficiency regime.

In summary, we are pursuing a three-step program to investigate nonlinear conversion into the mid infrared using diffusion-bonded GaAs stacks of plates and quasi-phase-matched nonlinear interactions. The program is staged to evolve from materials preparation to materials characterization followed by device testing. The device testing in turn will lead to improvements in all aspects of the nonlinear materials. The program also evolves from early experiments utilizing existing CO<sub>2</sub> laser to experiments that use 2- $\mu$ m, diode-pumped or lamp-pumped Tm:YAG solid-state lasers. The final part of the program explores the application of a high-average-power, Q-switched, mode-locked Nd:YAG laser as a driver for OPO/OPA conversion to 2- $\mu$ m followed by infrared generation by quasi-phase-matched difference-frequency mixing in diffusion-bonded GaAs stacks. The goal of this work is to demonstrate that the diffusion-bonded nonlinear materials will meet the requirements for application in high-peak-power and high-average-power mid-infrared sources of coherent optical radiation.

#### V. Relationship to Other Programs

The Army contract DAAL03-92-G-400 continues for another year, and work supported by this contract will focus on optimizing the diffusion-bonding process in GaAs. Much work remains to be done to understand the bonding conditions and to minimize the losses of the bonded stacks. This work will be aided by surface studies and process modeling. We will be bonding from 2 - 10 wafers, and will be using only SHG as a tool to evaluate the bonding. We are expecting a further year of support from the Office of Naval Research for work directed toward transitioning the ARO materials work into practical devices, and will break new ground in device demonstration. This report has been adapted from the proposal to ONR.

The proposed implementation of DBS QPM nonlinear mid-IR devices will benefit from other existing programs. The Center for Nonlinear Optical Materials (CNOM) at Stanford University was established one year ago under an ARPA University Research Initiative program. Professor Byer is the principal investigator for CNOM with Stanford faculty members Martin Fejer, James Harris, Robert Feigelson and Bert Hesselink. The goal of CNOM is to improve existing nonlinear bulk optical materials, and to develop integrated optical waveguide devices and photorefractive devices. We have established a CNOM Characterization Facility that will allow measurement of linear and nonlinear optical parameters. CNOM has also established a corporate Affiliates Program to enhance the interaction with industry on the commercial applications of nonlinear optical materials.

The investigation of diffusion-bonded-stacked GaAs for nonlinear infrared applications will benefit directly from access to the characterization facility. A number of companies have already expressed an interest in diffusion-bonded semiconductors, and the CNOM affiliates program provides a venue to exchange expertise and a way to use equipment currently unavailable at Stanford.

## VI. Scientific Personnel Supported by this Contract

### Principal Investigators

Professor Robert L. Byer	Applied Physics Department
Professor Robert S. Feigelson	Center for Materials Research

### Other Scientific Faculty and Staff

Martin M. Fejer	Assistant Professor, Applied Physics
Robert C. Eckardt	Sr. Research Associate, Ginzton Laboratory
Roger K. Route	Sr. Research Associate, Center for Materials Research

### Students

Leslie Gordon	Applied Physics
Sermon Wu	Materials Science and Engineering

## VI. References

1. L. Gordon, G. L. Woods, R. Route, R. S. Feigelson, R. C. Eckardt, M. M. Fejer, and R. L. Byer, "Diffusion bonded GaAs for SHG," in Conference on Lasers and Electro-Optics, (Optical Society of America, Washington, DC, 1993), pp. 38-39.
2. L. Gordon, G. L. Woods, R. C. Eckardt, R. K. Route, R. S. Feigelson, M. M. Fejer and R. L. Byer, "Diffusion bonded stacked GaAs for quasi-phase-matched second harmonic generation of a carbon dioxide laser," Electron. Lett. **29**, pp. 1942-1944 (1993).

3. J. A. Armstrong, N. Bloembergen, J. Ducuing, and P. S. Pershan, "Interactions between light waves in a nonlinear dielectric," *Phys. Rev.* **127**, pp. 1918-1939 (1962).
4. M. M. Fejer, G. A. Magel, D. H. Jundt, and R. L. Byer, "Quasi-phase-matched second harmonic generation: tuning and tolerances," *IEEE J. Quantum Electron.* **28**, pp. 2631-2654 (1992).
5. J. D. McMullen, "Optical parametric interactions in isotropic materials using a phase-corrected stack of nonlinear dielectric plates," *J. Appl. Phys.* **46**, pp. 3076-3081 (1975).
6. K. C. Rustagi, S. C. Mehendale and S. Mennakshi, "Optical frequency conversion in quasi-phase-matched stacks of nonlinear crystals," *IEEE J. Quantum Electron.* **QE-18**, pp. 1029-1041 (1982).
7. A. Szilagy, A. Hordvik and H. Schlossberg, "A quasi-phase-matching technique for efficient optical mixing and frequency doubling," *J. Appl. Phys.* **47**, pp. 2025-2032 (1976).
8. D. E. Thompson, J. D. McMullen and D. B. Anderson, "Second-harmonic generation in GaAs "stack of plate" using high-power CO<sub>2</sub> laser radiation," *Appl. Phys. Lett.* **29**, pp. 113-115 (1976).
9. E. J. Lim, M. M. Fejer and R. L. Byer, "Second-harmonic generation green light in periodically poled planar lithium niobate waveguide," *Electron. Lett.* **25**, pp. 174-175 (1989).
10. G. A. Magel, M. M. Fejer and R. L. Byer, "Quasi-phase-matched second-harmonic generation of blue light in periodically poled LiNbO<sub>3</sub>," *Appl. Phys. Lett.* **56**, pp. 108-110 (1990).
11. M. J. Angell, R. M. Emerson, J. L. Hoyt, J. F. Gibbons, M. L. Bortz, L. A. Eyres, and M. M. Fejer, "Orientation patterning of II-VI semiconductor films for quasi-phases-matched nonlinear devices," in *Integrat. Photon. Res. Technical Digest*, (Optical Society of America, Washington, DC, 1993), pp. 472-474.
12. H. Mao, F. Fu, B. Wu, and C.-T. Chen, "Noncritical quasiphase-matched second harmonic generation in LiB<sub>3</sub>O<sub>5</sub> crystal at room temperature," *Appl. Phys. Lett.* **61**, pp. 1148-1150 (1992).
13. J. J. Dudley, M. Ishikawa, D. I. Babic, B. I. Miller, R. Mirin, W. B. Jiang, J. E. Bowers, and E. L. Hu, "144°C operation of 1.3 μm InGaAsP vertical cavity lasers on GaAs substrates," *Appl. Phys. Lett.* **61**, pp. 3095-3097 (1992).
14. Z. L. Liao and D. E. Mull, "Wafer fusion: a novel technique for optoelectronic device fabrication and monolithic integration," *Appl. Phys. Lett.* **56**, pp. 737-739 (1990).
15. Y. H. Lo, R. Bhat, D. M. Hwang, M. A. Koza, and T. P. Lee, "Bonding by atomic rearrangement of InP/InGaAsP 1.5 μm wavelength lasers on GaAs substrates," *Appl. Phys. Lett.* **58**, pp. 1961-1963 (1991).

16. A. N. Pikhtin and A. D. Yas`kov, "Dispersion of the refractive index of semiconductors with diamond and zinc-blend structures," *Sov. Phys. Semicond.* **12**, pp. pp. 622-626 (1978).
17. S. J. Brosnan and R. L. Byer, "Optical parametric oscillator threshold and linewidth studies," *IEEE J. Quantum Electron.* **QE-15**, pp. 415-431 (1979).
18. G. D. Boyd and D. A. Kleinman, "Parametric interactions of focused Gaussian light beams," *J. Appl. Phys.* **39**, pp. 3597-3639 (1968).